Astronomy & Astrophysics manuscript no. landi˙fermi
June 25, 2015

Swift/XRT counterparts to unassociated *Fermi* high-energy LAT sources

R. Landi[1], L. Bassani[1], J. B. Stephen[1], N. Masetti[1], A. Malizia[1], and P. Ubertini[2]

[1] INAF/IASF Bologna, via Piero Gobetti 101, I–40129 Bologna, Italy
[2] INAF/IAPS Rome, Via Fosso del Cavaliere 100, I–00133 Rome, Italy

Received / accepted

ABSTRACT

We report the results from our analysis of a large set of archival data acquired with the X-ray telescope (XRT) onboard *Swift*, covering the sky region surrounding objects from the first *Fermi* Large Area Telescope (LAT) catalogue of high-energy sources (1FHL), which still lack an association. Of the 23 regions analysed, ten did not show any evidence of X-ray emission, but 13 were characterised by the presence of one or more objects emitting in the 0.3–10 keV band. Only in a couple of cases is the X-ray counterpart located outside the *Fermi* positional uncertainty, while in all other cases the associations found are compatible with the high-energy error ellipses. All counterparts we found have been studied in detail by means of a multi-waveband approach to evaluate their nature or class; in most cases, we have been able to propose a likely or possible association except for one *Fermi* source whose nature remains doubtful at the moment. The majority of the likely associations are extragalactic in nature, most probably blazars of the BL Lac type.

Key words. gamma-ray:general – X-ray:general

1. Introduction

A key strategic objective of the *Fermi* mission is to perform a survey of the sky at various gamma-ray energies. Recently, the first *Fermi*/LAT catalogue of high-energy sources (1FHL) has been published (Ackermann et al. 2013), listing 514 objects detected above 10 GeV. The main motivation behind this catalogue was to find the hardest gamma-ray sources in the sky and to get a sample of objects that are good candidates for detection at TeV energies. The vast majority of the sources reported therein could be immediately associated with known objects (449 or 87% of the sample): approximately 75% with active galactic nuclei (AGNs), mostly blazars, while Galactic sources, like pulsars, pulsar wind nebulae (PWNs), supernova remnants (SNRs), high-mass binaries, and star-forming regions, collectively represent 10% of the sample. The percentage of unassociated sources is less than 14% corresponding to 71 objects. The third *Fermi*/LAT catalogue (3FGL, Acero et al. 2015), which was subsequently published, contains most of these unassociated 1FHL sources except for 13 objects that are missing. Considering the associations discussed in the 3FGL catalogue (six objects) and our follow-up work (26 objects analysed by Landi et al. (2015a);(2015b)), the set of sources for which no counterpart has been found found contains at this stage 39 entries.

Identification of these objects is a primary objective of the mission, but it has been made difficult by the relatively large positional uncertainty (usually around a few arcminutes) of the *Fermi*/LAT instrument. Analysis of X-ray data can be a useful tool for restricting the positional uncertainty of the *Fermi* objects and facilitating the identification process. The list of likely counterparts that are found can then be studied in detail (for example using multi-waveband data) to identify those highly nusual objects with the parameters that might be expected to produce gamma-rays. Optical spectroscopy can finally be performed to confirm the association and classify the gamma-ray source.

Here we use data collected with the XRT instrument onboard the satellite *Swift* (Gehrels et al. 2004) to study a number of unassociated *Fermi* 1FHL sources. We do this by cross-correlating the list of 39 1FHL objects that lack a counterpart, with all the XRT pointings covering the *Fermi*/LAT positional uncertainty. Analysis of these data allows us to propose the likely or possible counterparts to another 12 *Fermi* high-energy objects; the nature of each likely or possible counterpart is studied by means of a multi-waveband approach and is generally found to conform to the nature of blazars of the BL Lac type.

2. *Swift*/XRT follow-up observations

We took all 39 sources in the 1FHL catalogue that still lack an association and class. The source positions were then cross-correlated with the *Swift*/XRT archival data, and we only considered distances between the *Fermi* source and XRT pointing positions below 9 arcmin in order to optimise coverage of the high-energy error ellipses. This cross-correlation method led to selecting a sample of 23 1FHL sources for which XRT data are available. The log of all X-ray observations analysed in this work is given in Table 1, where we report for each individual *Fermi* source, the XRT observation ID, the date and the exposure of the XRT pointings available up to March 15, 2015.

XRT data were reduced using the XRTDAS standard data pipeline package (XRTPIPELINE v. 0.12.9) to produce PC-mode screened event files. For each *Fermi* source, we summed together all the available XRT pointings using XSELECT v. 2.4c to enhance the signal-to-noise ratio and thus allow the detection of possible counterparts. The XRT images in the 0.3–10 keV energy band were obtained and analysed by means of the software package XIMAGE v. 4.5.1; some of the XRT images are shown in Figures from 1 to 4 and discussed in dedicated sections.

Send offprint requests to: landi@iasfbo.inaf.it

From the XRT data we did not find evidence of soft X-rays for ten sources in our sample and these are listed in Table 2, where we also quote an upper limit on the count rate in the 0.3–10 keV energy band and the Galactic neutral hydrogen column density in the source direction.

For each of the remaining objects, XRT detected one or more sources[1] in the region containing or surrounding the *Fermi* positional uncertainty. These cases are listed in Table 3 and discussed in the following sections. We also provide further X-ray information in Table 4: spectral parameters only for those sources for which the quality of the XRT data is good enough to perform a basic spectral analysis, i.e. a simple power law passing through Galactic absorption. In the remaining cases, we only estimate the 0.3–10 keV count rate and the Galactic neutral hydrogen column density in the source direction.

For the spectral analysis, source events were extracted within a circular region with a radius of 20 pixels (1 pixel ~ 2.36 arcsec) centred on the source position, while background events were extracted from a source-free region close to the X-ray source of interest. The spectra were obtained from the corresponding event files using the XSELECT v. 2.4c software and binned using GRPPHA in an appropriate way, so that the χ^2 statistic could be applied. We used version v.014 of the response matrices and created individual ancillary response files *arf* using XRTMKARF v. 0.6.0.

Finally, we point out that only four objects from Table 3 (1FHL J0639.6–1244, 1FHL J1240.4–7150, 1FHL J1507.0–6223, and 1FHL J1856.9+0252) are located close to the Galactic plane (i.e. below 10 degrees in Galactic latitude), suggesting that the remaining nine sources are most likely extragalactic.

3. Individual source studies

In the following, we provide detailed information available in the literature and in various archives on each individual association with the *Fermi* high-energy sources found in this work. Besides the X-ray information, we also checked the radio, infrared (by exploiting the Wide-field Infrared Survey Explorer (WISE, Wright et al. (2010)), and optical characteristics of each possible counterpart in order to understand its nature in more detail and to assess the likelihood of its association with the *Fermi* object. More specifically, in Table 3 we report, for each *Fermi* high-energy source for which we find one or more X-ray counterparts, the name, the number of X-ray sources detected with XRT in the corresponding fields (and next to it a reference number used in the WISE colour-colour plot (see Figure 5), their coordinates and error radius, the name of the WISE counterparts, its magnitudes ($W1$ = 3.5, $W2$ = 4.6, $W3$ = 12, $W4$ = 22 micron)[2], and the likelihood of association with the corresponding gamma-ray source. It is evident from Table 3 that the XRT location accuracy allows a significant reduction in the *Fermi* positional uncertainty, thus making the search for possible optical counterparts much easier.

In most cases, the soft X-ray error radius is lower than or equal to six arcseconds, i.e. sufficiently small to highlight only one optical counterpart. Also X-ray information as reported in Table 4 can be used to characterise each source, in particular the count rate, and the 2–10 keV flux can help to distinguish multiple counterparts. We used the WISE colours as discussed by Massaro et al. (2013a) to test the possible blazar nature of each source. These authors found that in the $W2 - W3$ versus $W1 - W2$ colour-colour plot the positions of gamma-ray emitting blazars are all within a well-defined region known as the "Blazar Strip". Therefore, objects with IR colours compatible with this strip could be AGN of the blazar type, hence be an even more likely counterpart to the *Fermi* high-energy sources. For the radio information, we either use data collected at 20 cm by the NRAO VLA Sky Survey (or NVSS, Condon et al. 1998), at 36 cm by the Sydney University Molonglo Sky Survey (or SUMSS, Mauch et al. 2003) and at 92 cm by the Westerbork Northern Sky Survey (or WENSS, Rengelink et al. 1997) or Westerbork In the Southern Hemishpere (or WISH, De Breuck et al. 2002).

We also consulted the results of Schinzel et al. (2015), who performed an All Sky survey between 5 (6) and 9 (3.3) GHz (cm) of sky areas surrounding unidentified objects listed in the second *Fermi*/LAT catalogue (2FGL, Nolan et al. 2012) in the search for new AGN associations with compact radio sources. Nine of our regions were covered by this survey, but only five were found to have a radio detection compatible with our proposed X-ray association. They are discussed in each individual section.

In the following, sources will be divided into three groups: those with a single counterpart, those with multiple associations within or at the border of the *Fermi* positional uncertainty, and those with a counterpart outside the *Fermi* error ellipse.

3.1. Single counterpart sources

In this section, we discuss those cases in which we find only one X-ray source inside the *Fermi* positional uncertainty. This information is used with the overall properties of the X-ray detection found to evaluate the likelihood of the association with the *Fermi* high-energy object.

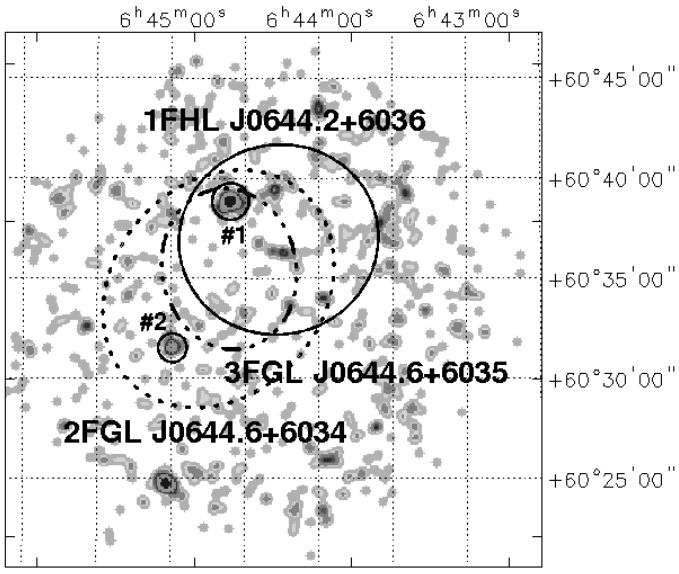

Fig. 1. XRT 0.3–10 keV image of the region surrounding 1FHL J0644.2+6036 (black ellipse)/2FGL J0644.6+6034 (black-dashed ellipse)/3FGL J0644.6+6035 (black-dashed-dotted ellipse). Source #1 is the only XRT detection compatible with the 1FHL J0644.2+6036 positional uncertainty. Source #2 represents the counterpart to 2FGL J0644.6+6034 discussed by Massaro et al. (2013b) and Paggi et al. (2014). A third source located outside both *Fermi* error ellipses is neither numbered nor discussed in the text.

[1] We have taken into account all XRT detections above 2.5σ confidence level.

[2] available at:
http://vizier.u-strasbg.fr/viz-bin/VizieR?-source=II%2F311.

3.1.1. 1FHL J0644.2+6036

The XRT counterpart found in this work (source #1 in Figure 1) is listed both in the NVSS (NVSS J064435+603849) and in the WENSS (B0640.0+6041) catalogues with 20 and 92 cm flux densities of ∼33.5 and ∼83 mJy, respectively (spectral index $\alpha = 0.6$)[3]. The WISE colours are $W2 - W3 = 1.97$ and $W1 - W2 = 0.64$, making this object compatible with the blazar strip. The high-energy *Fermi* source is also reported in the second /third*Fermi*/LAT catalogues as 2FGL J0644.6+6034/3FGL J0644.6+6035, an unidentified source studied by various authors. Massaro et al. (2013b) propose WISE J064459.38+603131.7 as the possible IR counterpart to 2FGL J0644.6+6034, while Paggi et al. (2013) find that this WISE source is also detected by *Swift*/XRT. Recently, Paggi et al. (2014) have provided the optical spectrum of this possible counterpart, finding that it could be a weak emission line quasar at $z = 0.3582$. As is evident in Figure 1, the positional uncertainties of 2FGL J0644.6+6034, 3FGL J0644.6+6035 and 1FHL J0644.2+6036 are partly overlapping. The error ellipse of 2FGL J0644.6+6034, apart from the source discussed by Massaro et al. (2013b) and Paggi et al. (2014) (source #2), contains also source #1 found in this work, while the error ellipse of 3FGL J0644.6+6035 contains only this XRT detection, which incidentally is also the brightest of the two X-ray emitters. The lack of any radio detection so far for source #2, combined with the above-mentioned characteristics of source #1, raise some questions about the reality of the association between WISE J064459.38+603131.7 and 2FGL J0644.6+6034, and suggest instead that source #1 is the only putative counterpart to the 2FGL, 3FGL, and 1FHL *Fermi* object. As a confirmation of our findings, we note that source #1 is also reported in the survey work by Schinzel et al. (2015) as a flat-spectrum compact radio source detected with a 6 cm flux density of ∼8.2 mJy.

3.1.2. 1FHL J1115.0–0701

This high-energy *Fermi* source has a counterpart in the still unclassified object 3FGL J1115.0–0701. The only XRT detection found is inside and at the border of the 1FHL and 3FGL error ellipse, respectively. The source has no radio counterpart or WISE colours ($W2 - W3 = 1.825$ and $W1 - W2 = 0.069$) that locate it outside the blazar strip. Both indications cast doubts on the association between this XRT detection and the *Fermi* high-energy source, which therefore we consider at this stage uncertain until optical follow-up observations provide a reliable classification of this X-ray source.

3.1.3. 1FHL J1129.2-7759

This XRT source has a counterpart in the *ROSAT* Bright (1RXS J113029.0–780108, 7 arcsec error radius) source catalogue (Voges et al. 1999), as well as in a *XMM-Newton* Slew survey catalogue (Saxton et al. 2008) (XMMSL1 J113031.6–780112, 3 arcsec error radius); indeed, its X-ray flux, listed in Table 4, is relatively high.

This X-ray source is most likely associated with the radio source PMN J1130–7801. The PMN object has a 36 cm flux density of ∼136 mJy and a flat ($\alpha = -0.4$) radio spectrum from 3.5 to 6 cm (McConnell et al. 2012). The source is also reported as a WISE object with the following IR colours: $W2 - W3 = 1.93$ and $W1 - W2 = 0.6$, which are fully compatible with the blazar strip. The source is discussed in a study of the Chamaeleon star-forming region (Alcala et al. 1995): it has been spectroscopically investigated, but unfortunately with no success. We also note that this X-ray/radio source falls within the positional uncertainty of the 3FGL counterpart (3FGL J1130.7–7800) of this 1FHL source.

3.1.4. 1FHL J1223.3+7953

This X-ray source is listed in the Two Micron All Sky Survey Extended sources catalogue (Skrutskie et al. 2006) as 2MASX J12235831+7953279 and was classified as a galaxy in NED. The source is also found in both the NVSS (NVSS J122358+795329) and WENSS (WN 1222.0+8010) catalogues with 20 and 92 cm flux densities of ∼31.5 and ∼43 mJy, respectively. A power-law fit between these two frequencies indicates a rather flat ($\alpha \sim 0.2$) radio spectrum. This is confirmed by the findings of Schinzel et al. (2015), who report parsec scale radio emission with a flat spectrum for this X-ray source. The WISE colours ($W2 - W3 = 1.92$ and $W1 - W2 = 0.48$) place the source well inside the blazar strip. This object is also listed in the Galaxy Evolution Explorer All-Sky Survey (GALEX, Bianchi et al. (2011)) as GALEXASC J122357.56+795328.7 with magnitudes of 24.6 and 22.3 in the far- and near-UV. Massaro et al. (2015) have recently identified it as a BL Lac of unknown redshift. We note that this 1FHL source is listed as 3FGL J1222.7+7952 in the third *Fermi* catalogue, and the XRT source lies at the border of its positional uncertainty confirming 2MASX J12235831+7953279 as the counterpart to both gamma-ray detections.

3.1.5. 1FHL J1240.4–6150

The 3FGL association for this source is 3FGL J1240.3–7149. The only XRT source found is inside the error ellipses of both 1FGH and 3FGL objects. It is associated with the *XMM-Newton* object XMMSL1 J124021.7–714854 (2.0 arcsec error radius) and displays a relatively high X-ray flux (see Table 4). It has a radio counterpart (MGPS J124021–714901) that shows a ∼15.5 mJy flux density at 36 cm (Murphy et al. 2007) and a flat radio spectrum between 5 and 9 GHz ($\alpha = -0.45$, Petrov et al. 2013). In this case Schinzel et al. (2015) report parsec scale radio emission emission with 6 and 3.3 cm flux densities of ∼14 and ∼11.2 mJy, respectively ($\alpha = 0.3$) for this X-ray source. The source is listed in the WISE catalogue with colours $W2 - W3 = 1.34$ and $W1 - W2 = 0.52$, which places it outside the blazar strip.

3.1.6. 1FHL J1315.7–0730

In this case, the XRT source is associated with a relatively weak radio source (NVSS J131552–073301), displaying a 20 cm flux density of ∼23.8 mJy and a flat ($\alpha \sim -0.1$) radio spectrum (Petrov et al. 2013). Radio emission is also reported by Schinzel et al. (2015) with 6 and 3.3 cm flux densities of ∼40.2 and ∼38.4 mJy, respectively, confirming the flat radio spectrum. This source is WISE-detected with colours $W2 - W3 = 2.27$ and $W1 - W2 = 0.88$, which are again compatible with those of gamma-ray emitting blazars. In UV the source can be associated with a GALEX object (GALEXASC J131553.03–073302.4), which displays variability and high polarization (Bauer et al. 2009; Fujiwara et al. 2013). On the basis of these peculiarities, Massaro et al. (2013b) suggest that it could be a new gamma-ray blazar, while Hassan et al. (2013) conclude that it might be a

[3] Here and in the following, we use $S \propto \nu^{\alpha}$, where S is the flux density, ν is the frequency, and α the spectral index.

BL Lac object. This 1FHL source is reported as 3FGL J1315.7–0732 in the third *Fermi* catalogue. Our XRT detection lies well within the 3FGL positional uncertainty, thus also confirming our proposed association for the lower energy gamma-ray emitter.

3.1.7. 1FHL J1507.0–6223

The only X-ray source detected by XRT lies on the border of the *Fermi* error ellipse and has no radio counterpart. Furthermore, the WISE colours $W2 - W3 = 1.17$ and $W1 - W2 = -0.011$ place this source well outside the blazar strip. In the third *Fermi* catalogue, this source is reported as an unclassified source that is nevertheless associated with HESS J1507–622. The three error ellipses (1FHL, 3FGL, and HESS) overlap considerably, but the smaller positional uncertainty of the third *Fermi* catalogue excludes the XRT object as a possible counterpart. This sky region has been studied in depth at X-rays energies using *Chandra*, *XMM-Newton*, and *Suzaku* (Tibolla et al. 2014; Eger et al. 2015) data. These observations, which are by far more sensitive than ours, revealed several X-ray sources, but not the XRT one discussed here. This lack of detection may be due either to source variability or to different exposure times. Of the two sources that are compatible with the restricted 3FGL error ellipse, one (source X3, Figure 1 in Tibolla et al. 2014) is a star and the other (source S6, Figure 1 in Eger et al. 2015) is too faint for an in-depth analysis.

At the present stage the most accredited association with HESS 1507–622 is a faint extended X-ray source thought to be a PWN; although this source is at the border of the HESS and 1FHL positional uncertainties, it is well outside the 3FGL ellipse, which casts some doubt on its true association with the MeV/TeV object. This source clearly deserves further study, but on the basis of the above information, we consider the association between the XRT and the *Fermi* high-energy source unlikely.

3.2. ***Multiple counterpart sources***

In the following cases, more than one single X-ray detection is found within the *Fermi* error ellipse. Although this makes things more difficult to handle, it is still possible to highlight a more likely association on the basis of a multi-waveband approach.

3.2.1. 1FHL J0746.3–0225

This is a case where there are two X-ray detections inside the *Fermi* error ellipse (see upper left panel of Figure 2), but only one (source #1), which is the brightest, is a likely counterpart. It is in fact the only one with radio emission because it is listed in the NVSS survey as NVSS J074627–022549, with a 20 cm flux density of ∼12.8 mJy. It has a WISE counterpart with colours $W2 - W3 = 2.1$ and $W1 - W2 = 0.68$, as is typical of gamma-ray blazars. This X-ray source is also UV-detected (GALEXASC J074627.06–022548.9) with far- and near-UV magnitude in the range 20.4–20.8. The other object is dimmer, has no interesting association in other catalogues, and is therefore a less likely association. In the latest *Fermi* catalogue, 1FHL J0746.3–0225 is associated with 3FGL J0746.4–0225; as is clear in Figure 2, the 3FGL error ellipse confirms the association of the high-energy detection with source #1 and excludes source #2 as a possible counterpart.

3.2.2. 1FHL J1410.4+7408

Also in this case we find a couple of detections that are compatible with the 1FHL positional uncertainty (see upper right panel of Figure 2). Both have WISE colours ($W2 - W3 = 2.79$ and $W1 - W2 = 0.88$ and $W2 - W3 = 1.81$ and $W1 - W2 = 0.79$ for #1 and #2, respectively), so just compatible with the blazar strip, but no detection in radio. We also note that within the 1FHL positional uncertainty, there is also a *XMM-Newton* Slew source XMMSL1 J141002.6+740744 (5 arcsec error radius), which is quite bright in X-rays (0.2–12 keV flux of 2.3×10^{-12} erg cm^{-2} s^{-1}); despite this, we could not find a radio, infrared, or optical counterpart, even when doubling its positional uncertainty. Only going to an 18 arcsec distance are we able to find an association with a WISE object. Its WISE magnitudes are $W1 = 17.189$, $W2 = 16.771$, $W3 = 12.792$ and $W4 = 9.606$, and its colours turn out to be $W2 - W3 = 3.98$ and $W1 - W2 = 0.42$, which locate the source outside the blazar strip. Also this counterpart is not reported at radio frequencies. That this *XMM-Newton* Slew source is detected in neither the combined XRT image nor the individual observations, indicates further that it is extremely variable in X-rays. Despite its potential interest, this *XMM-Newton* Slew detection is, however, outside the error ellipse of the 3FGL counterpart of this high-energy *Fermi* source. The other two X-ray sources are instead both well inside the 3FGL positional uncertainty, so are more likely candidates. Clearly, this is another complicated case, and only optical follow-up observations can help to identify which of these two (possibly three) X-ray detections is the true counterpart to this high-energy emitter.

3.2.3. 1FHL J2134.6–2130

In this case three XRT sources are found within the 1FHL error ellipse (see lower left panel of Figure 2). Source #1 has a radio counterpart (NVSS J213430–213032) with a 20 cm flux density of ∼22 mJy and a flat radio index of 0.23 (Petrov et al. 2013). It is also reported in the list of possible compact radio counterparts to 2FGL sources by Schinzel et al. (2015), where it is described as a flat spectrum source with 6 and 3.3 cm flux densities of ∼92.8 and ∼103.9 mJy, respectively. The WISE colours ($W2 - W3 = 2.27$ and $W1 - W2 = 0.78$) are just compatible with the blazar strip and the source is discussed by various authors as a possible counterpart to 2FGL J2134.6–2130; for example, Massaro et al. (2013b) and Hassan et al.(2013) suggest that it could be a blazar of the BL Lac type. Source #2 is listed as a galaxy in NED, but it has no detection in radio, and it does not display WISE colours typical of blazars, so we consider it an unlikely association. As for source #3, the lack of any radio counterpart, as well as of WISE colours ($W2 - W3 = 3.213$ and $W1 - W2 = 0.481$) that are not compatible with the blazar strip, suggests that this object is also an unlikely association. The third *Fermi* catalogue lists this object as 3FGL J2134.5–2131. Its restricted error ellipse excludes source #3 as a likely counterpart, but maintains #1 and #2 as possible associations. On the basis of our analysis, we consider only the first to be the most promising counterpart to this *Fermi* high-energy detection.

3.2.4. 1FHL J2257.9–3644

Only two soft X-ray counterparts are found within the *Fermi* error ellipse (see lower right panel of Figure 2). This 1FHL source is listed in the 3FGL catalogue as 3FGL J2258.2–3645. Even though its positional uncertainty is smaller than in the 1FHL survey, it does not help to exclude one of the two X-ray detec-

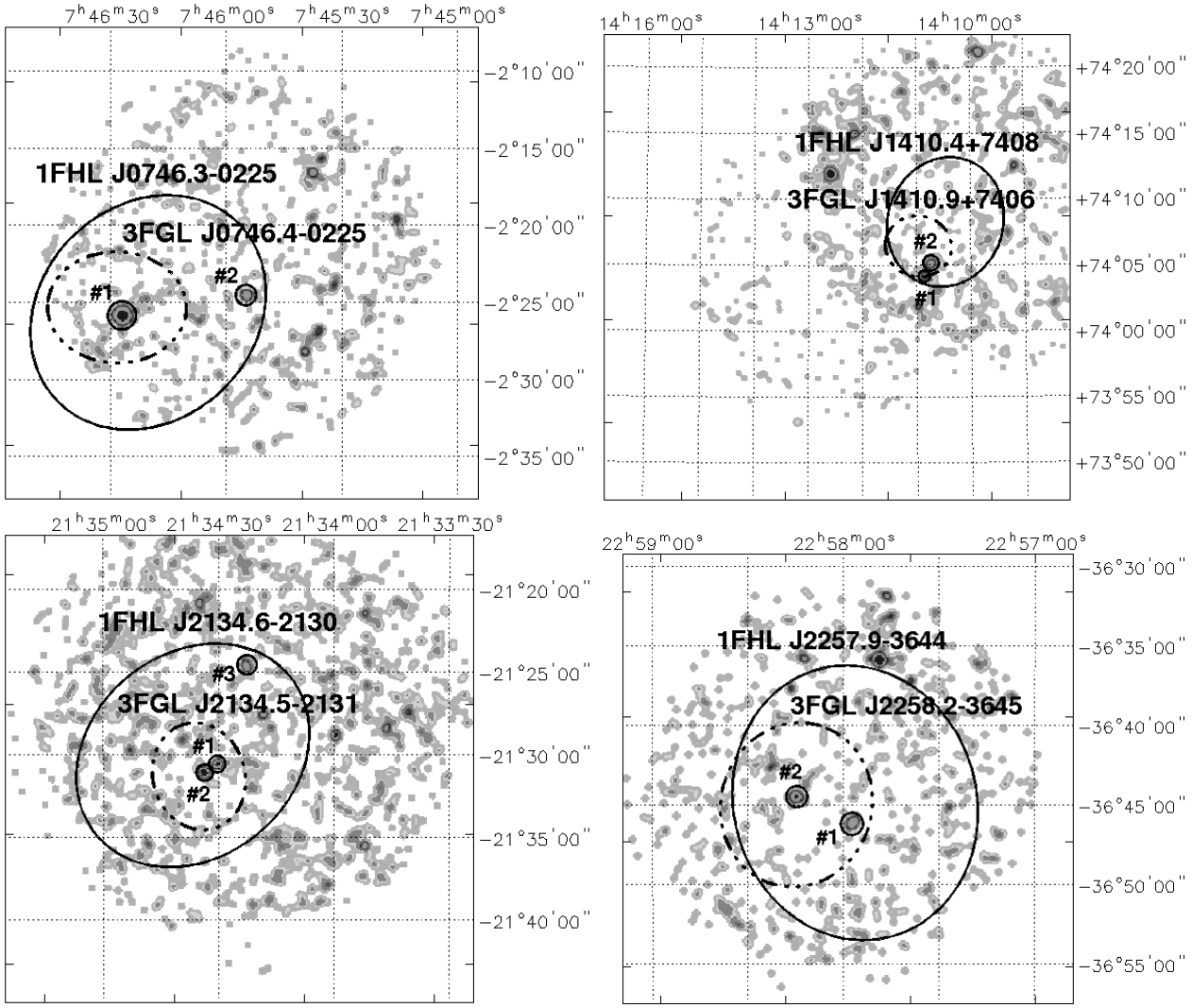

Fig. 2. XRT 0.3–10 keV images of high-energy *Fermi* sources for which more than one X-ray detection is found. Black circles depict the location of each XRT detection. Black ellipse and black-dashed-dotted ellipse depict the positional uncertainty of the 1FHL and 3FGL sources, respectively.

tions. Source #1 is dim with no counterparts in radio catalogues and WISE colours $W2 - W3 = 3.06$ and $W1 - W2 = 1.46$, which locate the source at the upper border of the blazar strip. The other detection (source #2 in the figure) is brighter and has a radio detection in the NVSS (NVSS J225815–364433) and in the SUMSS (SUMSS J225816–364446) with 20 and 36 cm flux densities of ∼10.6 and ∼14.1 mJy, respectively. The radio spectrum is quite flat displaying an index of 0.23 (Petrov et al. 2013). The source is also reported in the WISE catalogue with colours $W2 - W3 = 2.24$ and $W1 - W2 = 0.57$, which are compatible with the blazar strip. It is also listed in the GALEX All-Sky survey (GALEXASC J225815.00–364434.6) with far- and near-UV magnitudes around 20–21. Source #2 is reported as a galaxy in NED and has recently been classified as a BL Lac by Landoni et al. (2015). Optical spectroscopy of source #1 could unambiguously exclude it as the counterpart of this *Fermi* high-energy emitter.

3.3. ***Objects with X-ray detection outside the Fermi positional uncertainty***

In two cases (1FHL J0639.6–1244 and 1FHL J1856.9+0252), we find a bright X-ray source outside the *Fermi* error ellipse. Despite this, in each case the association may be considered at least interesting for a number of reasons: a) *Fermi* error ellipses are quoted at the 95% confidence level, which suggests that in 5% of the cases, the true counterpart could be located outside; b) the associations are with interesting objects, which may have the characteristics of gamma-ray emitting objects; c) there is nothing else inside the *Fermi* positional uncertainty that could be of potential interest.

3.3.1. 1FHL J0639.6–1244

The only X-ray detection lies around 11 arcmin away from the *Fermi* position (see Figure 3). This object is associated with 2MASX J06400717–1253150 and with the flat spectrum radio object PMN J0640–1253 ($\alpha \sim -0.4$, Chhetri et al. 2013). This source is fairly bright in radio with a 20 cm flux density of ∼225 mJy and is detected by WISE with colours ($W2 - W3 = 1.74$ and

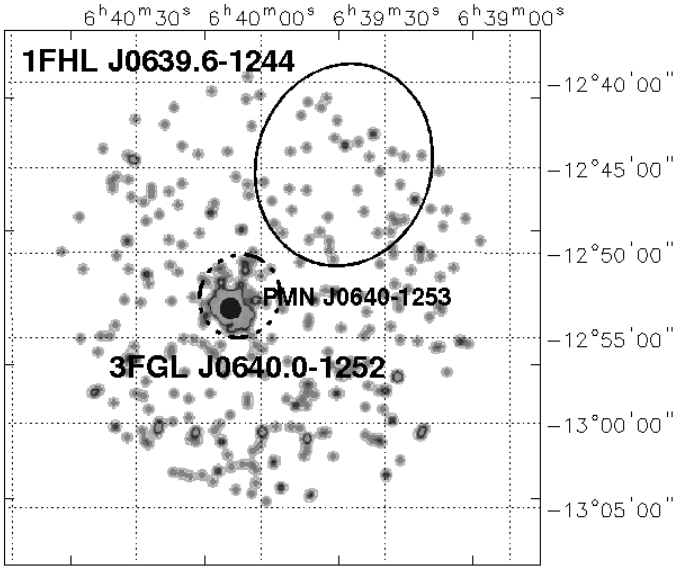

Fig. 3. XRT 0.3–10 keV image of the region surrounding 1FHL J0639.6–1244 (black ellipse). The only X-ray object detected by XRT, namely PMN J0640–1253, lies ∼5 arcmin away from the border of *Fermi* positional uncertainty, but is found to be within the error ellipse of 3FGL J0640.0–1252 (black-dashed-dotted ellipse).

$W1 - W2 = 0.457$), which are once again fully compatible with the blazar strip. It is also quite bright in X-rays (see Table 4), thus strengthening its association with 1FHL J0639.6–1244.

It was proposed as a BL Lac candidate for TeV emission by Massaro et al. (2013b). The nearest 3FGL source is 3FGL J0640.0–1253, but the two *Fermi* detections are not associated in the 3FGL catalogue, given that their positional uncertainties do not overlap (see Figure 3). As is evident from the figure, the 3FGL source is associated with PMN J0640–1253. Seeing as there is no other X-ray emitter in this zone and that the 3FGL source could be expected to radiate even above 10 GeV, it is possible that the 1FHL error circle is slightly underestimated and then the two *Fermi* objects could well be the same source. We therefore consider the association possible.

3.3.2. 1FHL J1856.9+0252

This source is not reported in the third *Fermi* catalogue. As displayed in Figure 4, it is not far from the TeV emitter HESS J1857+026, which is generally classified as a PWN candidate (Acero et al. 2013); the morphology and overall spectral shape of the main emission zone, combined with the proximity to the pulsar PSR J1856+0245 (Hessels et al. 2008), support this classification.

Unfortunately, the two error ellipses (from *Fermi* and from TeV observations) do not overlap, which makes the possible association between the two wavebands uncertain. Nearby the *Fermi* error ellipse XRT detects source #1 whose WISE colours ($W2 - W3 = 1.91$ and $W1 - W2 = 1.71$) locate it well outside the blazar strip; furthermore, this object has no counterpart in radio surveys. A second source (#2 in Figure 4) coincides with the pulsar PSR J1856+0245, which is thought to be responsible for the HESS emission. It is difficult at this stage to conclude which of the two sources is the true association with the 1FHL object, nor is it clear whether the HESS and *Fermi* detection are the same object, leaving this case unresolved. For the following, we consider source #1 as the possible association.

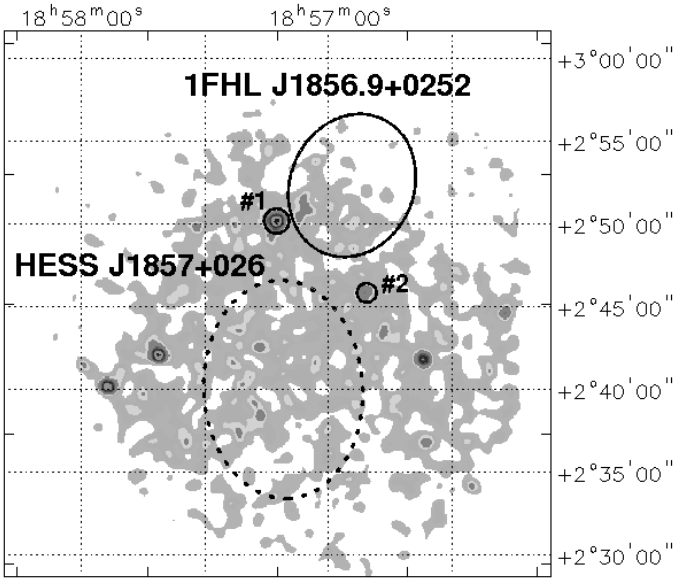

Fig. 4. XRT 0.3–10 keV image of the region surrounding 1FHL J1856.9+0252 (black ellipse). Source #1 and #2 are the sources detected by XRT in the region surrounding the *Fermi* object. Source #2 coincides with the pulsar PSR J1856+0245, which has been suggested to power the HESS object (black-dotted ellipse).

4. Discussion and conclusion

The first result of this work is that we have uncovered a number of likely X-ray counterparts to still unassociated 1FHL gamma-ray sources. The majority of these associations are likely to be extragalactic in nature, most probably blazars of some type. Only in the case of 1FHL J1115.0–0701 is the association considered to be unlikely. In four other cases, the proposed associations are to be taken as possible. More specifically, for 1FHL J1115.0–0701 and 1FHL J1410.4+7408, the X-ray detections are compatible with the 1FHL positional uncertainty, but the overall multi-wavelength properties prevent us from drawing any firm conclusions about their nature and only future optical follow-up observations can help to provide a reliable classification of these X-ray sources. In the other two cases (1FHL J0639.6–1244 and 1FHL J1856.9+0252), the X-ray detection lies outside the 1FHL error ellipse. For 1FHL J0639.6–1244, there is only one bright X-ray source detected in the region surrounding the 1FHL source, which coincides with PMN J0640–1253, a flat spectrum radio source that has been recently associated with the third *Fermi* catalogue source 3FGL J0640.0–1252. Although the 1FHL and 3FGL error ellipses do not overlap, we suggest that a likely association between PMN J0640–1253 and the 1FHL source cannot be ruled out. Also in the case of 1FHL J1856.9+0252 the overall multi-waveband properties of the only XRT detection do not allow us to associate firmly the X-ray source with the 1FHL object.

In the remaining cases, at least one of the proposed associations has a radio detection and WISE colours compatible with the blazar strip, in other words, it qualifies as beamed AGN. Indeed two objects (1FHL J1223.3+7953 and 1FHL J2257.9–

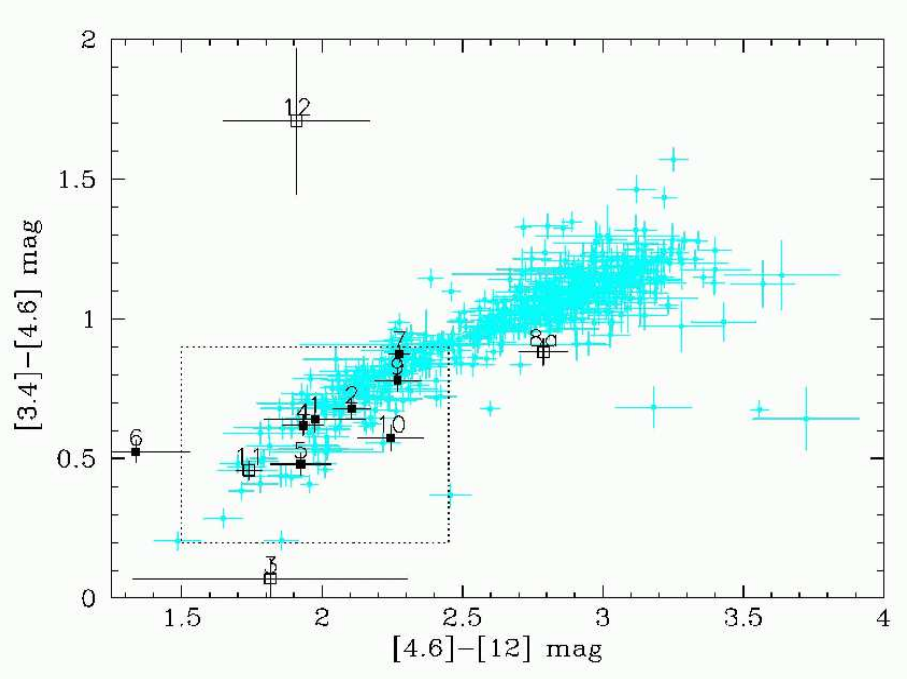

Fig. 5. [4.6]–[12]/[3.4]–[4.6] MIR colour-colour plot reporting the positions of gamma-ray emitting blazars (in cyan) associated with WISE sources forming the blazar strip (see Massaro et al. (2013a) for more details), together with the BL Lac objects identified in this paper. Filled and unfilled squares depict the proposed associations flagged with *L* or *P* in the last column of Table 3, respectively.

3644) have been optically classified as BL Lac objects. As already noted by Stephen et al. (2010) and confirmed by Masetti et al. (2013), the association of *Fermi* sources with soft X-ray counterparts favours discovery of this type of blazar. The preference for finding BL Lac when using soft X-ray data is very likely related to the SED of these objects compared to flat spectrum radio quasars. In fact, the X-ray selection favours the discovery of high synchrotron peaked or HSP blazars, which are also good candidates for TeV emission, because the Compton peak in these AGN is expected in this energy range owing to the presence of high-energy electrons.

As discussed by Masetti et al. (2013) and in the references therein, these objects populate a well-defined region of the WISE colour-colour diagram, i.e a square located in the lower part of the blazar strip. In fact, if we plot in the WISE colour-colour diagram (see Figure 5), the most likely counterparts to 1FHL sources listed in Table 3 (i.e. considering only those sources flagged with *L* or *P* in the last column of the Table), we notice that most fall along the blazar strip or close to it but, most important, nine of them lie within the limits of the locus populated by TeV-emitting BL Lacs, while one is at its border. Of the two possible counterparts of 1FHL J1410.4+7408, one lies within the TeV square (8b), while the other is on the blazar strip (8a), thus suggesting that both are likely associations. Finally, Figure 5 confirms that the association proposed here for 1FHL J1856.9+0252 (#12 in the figure) remains highly uncertain. We therefore conclude once again that the association among unassociated high-energy *Fermi* sources and soft X-ray objects appears to select blazars, for a large percentage of the HSP BL Lac type, i.e. those that are good candidates for TeV emission. Clearly, only the optical spectroscopy of all soft X-ray counterparts discussed in this work can confirm this suggestion and provide further insight into gamma-ray selected blazars in general and BL Lac in particular.

Acknowledgements. This research made use of the NASA/IPAC Extragalactic Database (NED) operated by the Jet Propulsion Laboratory (California Institute of Technology) and of the HEASARC archive provided by NASA's Goddard Space Flight Center. The authors also acknowledge the use of public data from the *Swift* data archive. R. L. acknowledges financial support under contract INTEGRAL ASI I/033/10/0. N. M. thanks Francesco Massaro for help with the preparation of Figure 5.

References

Acero, F., Ackermann, M., Ajello, M., et al. 2015, ApJS, 218, 23
Acero, F., Ackermann, M., Ajello, M., et al. 2013, ApJ, 773, 77
Ackermann, M., Ajello, M., Allafort, A., et al. 2013, ApJS, 209, 34
lcala, J. M., Frasca, A., Spezzi, L., et al. 1005, Mem. S.A.It, 76, 241
Bauer, A., Baltay, C., Coppi, P., et al. 2009, ApJ, 705, 46
Bianchi, L., Herald, J., Efremova, B., et al. 2011, Ap&SS, 335, 161
Chhetri, R., Ekers, R. D., Jones, P. A., Ricci, R. 2013, MNRAS, 434, 956
Condon, J. J., Cotton, W. D., Greisen, E. W., et al. 1998, AJ, 115, 1693
De Breuck, C., Tang, Y., de Bruyn, A. G., Röttgering, H, van Breugel, W. 2002, A&A, 394, 59
Eger, P., Domainko, W. F., Hahn, J. 2015, MNRAS, 477, 3564
Fujiwara, M., Matsuoka, Y., Ienaka, N., et al. 2012, AJ, 144, 112
Gehrels, N., Chincarini, G., Giommi, P., et al. 2004, ApJ, 611, 1005
Hassan, T., Mirabal, N., Contreras, J. L., Oya, I. 2013, MNRAS, 428, 220
Hessels, J. W. T., Nice, D. J., Gaensler, B. M., et al. 2008, ApJ, 682, L41
Landi, R., Bassani, L., Stephen, J. B., et al. 2015a, INAF/IASF Bologna, Internal report n. 651/2015
Landi, R., Bassani, L., Stephen, J. B., et al. 2015b, Proc. of "*Swift*: 10 years of discovery", 2–5 December 2014, La Sapienza University, Rome, Italy, in Proceedings of Science (SWIFT 10), arXiv:1506.07006
Landoni, M., Massaro, F., Paggi, A., et al. 2015, AJ, 149, 163
Masetti, N., Sbarufatti, B., Parisi, P., et al. 2013, A&A, 559, A58
Massaro, F., Landoni, M., D'Abrusco, R., et al. 2015, A&A, 575, A124
Massaro, F., D'Abrusco, R.; Paggi, A., et al. 2013a, ApJS, 209, 13
Massaro, F., D'Abrusco, R.; Paggi, A., et al. 2013b, ApJS, 206, 13
Mauch, T., Murphy, T., Buttery, H. J., et al. 2003, MNRAS, 342, 1117
Murphy, T., Mauch, T., Green, A., et al. 2007, MNRAS, 382, 382
McConnell, D., Sadler, E. M., Murphy, T., Ekers, R. D. 2012, MNRAS, 422, 1527
Nolan, P. L., Abdo, A. A., Ackermann, M., et al. 2012, ApJS, 199, 31
Paggi, A., Milisavljevic, D., Masetti, N., et al. 2014, AJ, 147, 112
Paggi, A., Massaro, F., D'Abrusco, R., et al. 2013, ApJS, 209, 9

Petrov, L., Mahony, E. K., Edwards, P. G., et al. 2013, MNRAS, 432, 1294
Rengelink, R. B., Tang, Y., de Bruyn, A. G., et al. 1997, A&AS, 124, 259
Saxton, R. D., Read, A. M., Esquej, P., et al. 2008, A&A, 480, 611
Schinzel, F. K., Petrov, L., Taylor, G. B., et al. 2015, ApJS, 217, 4
Skrutskie, M. F., Cutri, R. M., Stiening, R., et al. 2006, AJ, 131, 1163
Stephen, J. B., Bassani, L., Landi, R., et al. 2010, MNRAS, 408, 422
Tibolla, O., Kaufmann, S., Kosack, K. 2014, A&A, 567, A74
Voges, W., Aschenbach, B., Boller, Th., et al. 1999, A&A, 349, 389
Wright E.L., Eisenhardt, P. R. M., Mainzer, A. K., et al. 2010, AJ, 140, 1868

Table 1. Log of the *Swift*/XRT observations used in this paper (until March 15, 2015).

Fermi source	ID	Obs date	Exposure (s)
1FHL J0312.8+2013	00047145001	Jul 01, 2012	2186
	00047145002	Jul 05, 2012	1645
	00047145003	Jul 07, 2012	281
total obs	–	–	4112
1FHL J0625.9+0002	00041322001	Aug 23, 2010	2516
	00041322002	Sep 08, 2010	1868
total obs	–	–	4384
1FHL J0639.6–1244	00083670001	Feb 27, 2014	711
1FHL J0644.2+6036	00047166002	Feb 09, 2012	1494
	00047166003	Feb 13, 2012	1762
total obs	–	–	3256
1FHL J0746.3–0225	00047174002	Feb 25, 2012	2940
	00047174003	Nov 05, 2012	1408
total obs	–	–	4348
1FHL J0928.1–5252	00084691001	Feb 05, 2015	116
	00084691002	Feb 09, 2015	1597
	00084691003	Feb 15, 2015	133
	00084691004	Apr 03, 2015	83
total obs	–	–	1929
1FHL J1115.0–0701	00047198001	Jan 24, 2012	718
	00047198002	Mar 20, 2012	699
	00047198004	Mar 29, 2012	672
	00047198006	Jun 22, 2012	1296
total obs	–	–	3385
1FHL J1129.2-7759	00084723001	Feb 03, 2015	276
	00084723002	Feb 04, 2015	231
	00084723003	Feb 05, 2015	448
	00084723004	Feb 07, 2015	293
	00084723005	Feb 08, 2015	905
	00084723006	Feb 15, 2015	662
	00084723007	Mar 06, 2015	602
total obs	–	–	3417
1FHL J1223.3+7953	00047201001	Feb 10, 2012	4179
1FHL J1240.4–7150	00041386001	Feb 12, 2011	3161
	00041386002	Feb 14, 2011	1605
total obs	–	–	4766
1FHL J1315.7–0730	00041395001	Aug 18, 2010	4958
	00041395002	Aug 21, 2010	1678
total obs	–	–	6636
1FHL J1407.1–6133	00042321001	Mar 10, 2012	617
1FHL J1410.4+7408	00041402001	Mar 08, 2011	1414
	00041402003	Mar 11, 2011	2007
	00047219004	Mar 29, 2012	1026
	00047219006	Apr 05, 2012	1171
	00084043009	Jun 12, 2014	1258
total obs	–	–	6876
1FHL J1507.0–6223	00047226002	Dec 18, 2012	2009
	00047226003	Dec 19, 2012	1826
total obs	–	–	3835
1FHL J1619.8+7540	00084770001	Jan 23, 2015	756
1FHL J1634.7–4705	00042964002	Jan 16, 2012	341
	00410087000	Jan 29, 2012	516
	00042957001	Apr 28, 2012	543
	00080704001	Mar 12, 2014	788
	00080705001	Mar 12, 2014	2059
total obs	–	–	4247
1FHL J1758.3–2340	00049691001	Jun 28, 2014	203
	00043785001	Oct 05, 2012	513
total obs	–	–	716
1FHL J1839.1–0557	00044397001	Mar 15, 2013	527
1FHL J1839.4–0708	00044371001	Mar 15, 2013	528

Source	ID	Obs date	Exposure (s)
1FHL J1856.9+0252	00036183001	Nov 10, 2006	720
	00036184001	Mar 01, 2007	3097
	00036184002	Mar 07, 2007	4107
	00036183002	Mar 13, 2007	4102
	00037742001	Nov 16, 2008	9148
	00044642002	Mar 02, 2013	456
	00032774001	Mar 27, 2013	782
	00032782001	Mar 28, 2013	782
total obs	–	–	23194
1FHL J2004.4+3339	00041467001	Sep 05, 2010	448
	00041467002	Jan 09, 2011	1605
	00041467004	Jan 16, 2011	2040
total obs	–	–	4093
1FHL J2134.6–2130	00041496001	Sep 26, 2010	439
	00041496002	Dec 19, 2010	1838
	00041496003	Dec 23, 2010	4274
	00084044001	Jul 27, 2014	1304
	00084044002	Aug 05, 2014	1036
	00084044003	Sep 12, 2014	156
	00084044004	Sep 14, 2014	453
	00084044005	Oct 13, 2014	739
	00084044006	Oct 15, 2014	273
	00084044008	Dec 18, 2014	1203
total obs	–	–	11715
1FHL J2257.9–3644	00041507001	Aug 02, 2010	1734
	00041507002	Aug 12, 2010	1800
total obs	–	–	3534

Table 2. High-energy *Fermi* sources for which we do not find any X-ray counterpart.

Fermi source	Count rate[†] (10^{-3} counts s^{-1})	$N_{H(Gal)}$ (10^{22} cm^{-2})
1FHL J0312.8+2013	< 2.71	0.0988
1FHL J0625.9+0002	< 1.80	0.413
1FHL J0928.1–5252	< 4.00	0.938
1FHL J1407.1–6133	< 14.7	2.00
1FHL J1619.8+7540	< 0.67	0.0382
1FHL J1634.7–4705	< 0.65	1.68
1FHL J1758.3–2340	< 0.44	1.12
1FHL J1839.1–0557[‡]	< 0.59	1.74
1FHL J1839.4–0708	< 0.39	1.44
1FHL J2004.4+3339	< 0.98	1.15

[†] Count rates are extracted in the 0.3–10 keV energy band;
[‡] Source in the field of HESS J1841–055.

Table 3. List of the XRT detections and their WISE properties found for each high-energy *Fermi* source.

Fermi source	XRT source†				WISE counterpart					Association‡
	Source	R.A. (J2000)	Dec. (J2000)	error (arcsec)	Name	Magnitudes W1[3.4 μm]	W2[4.6 μm]	W3[12 μm]	W4[22 μm]	
1FHL J0644.2+6036	single(1)	06 44 36.48	+60 38 49.40	4.2	WISE J064435.72+603851.2	14.272	13.631	11.657	9.246	**L**
1FHL J0746.3–0225	#1(2)	07 46 27.14	–02 25 50.70	3.7	WISE J074627.03–022549.3	13.090	12.413	10.308	8.314	**L**
	#2	07 45 54.93	–02 24 31.40	4.4	WISE J074554.80–022430.7	15.559	14.501	11.974	8.968	U
1FHL J1115.0–0701	single(3)	11 15 15.30	–07 01 26.00	6.0	WISE J111515.34–070125.7	14.428	14.359	12.534	8.561	**P**
1FHL J1129.2-7759	single(5)	11 30 32.25	–78 01 05.20	3.6	WISE J113031.99–780105.5	13.323	12.705	10.772	8.828	**L**
1FHL J1223.3+7953	single(4)	12 23 59.71	+79 53 24.40	5.1	WISE J122358.17+795327.8	13.871	13.391	11.467	9.236	**L**
1FHL J1240.4–7150	single(6)	12 40 21.34	–71 48 58.51	3.6	WISE J124021.21–714857.7	13.396	12.871	11.534	8.648	**L**
1FHL J1315.7–0730	single(7)	13 15 53.06	–07 33 01.80	3.6	WISE J131552.98–073301.9	12.371	11.496	9.221	7.185	**L**
1FHL J1410.4+7408	#1(8a)	14 10 52.10	+74 04 14.40	6.0	WISE J141052.02+740415.1	14.872	13.991	11.203	9.029	**P**
	#2(8b)	14 10 45.40	+74 05 10.40	6.0	WISE J141046.01+740511.2	14.850	14.051	12.233	9.153	**P**
1FHL J1507.0–6223	single	15 07 59.00	–62 25 21.80	6.0	WISE J150758.80–622526.9	12.187	12.198	11.027	8.254	U
1FHL J2134.6–2130	#1(9)	21 34 30.40	–21 30 33.00	5.0	WISE J213430.18–213032.6	13.548	12.768	10.499	8.717	**L**
	#2	21 34 33.31	–21 31 05.30	5.6	WISE J213433.41–213103.2	15.238	14.728	11.582	8.725	U
	#3	21 34 22.60	–21 24 33.50	6.0	WISE J213423.04–212435.6	16.179	15.698	12.485	9.027	U
1FHL J2257.9–3644	#1	22 57 57.38	–36 46 11.90	4.9	WISE J225757.06–364608.5	15.342	13.880	10.824	8.520	U
	#2(10)	22 58 14.74	–36 44 28.80	5.1	WISE J225815.00–364434.2	13.860	13.287	11.042	8.916	**L**
Objects with X-ray detection outside the *Fermi* positional uncertainty										
1FHL J0639.6–1244	single(11)	06 40 07.31	–12 53 18.60	3.8	WISE J064007.19–125315.0	11.891	11.434	9.694	7.745	**P**
1FHL J1856.9+0252	single(12)	18 57 12.70	+02 50 11.30	3.3	WISE J185712.64+025007.8	14.253	12.545	10.637	7.299	**P**

† The number in parenthesis next to the XRT sources flagged either with *L* or *P* in the last column of the Table is a reference used in the WISE colour-colour plot (see Figure 5 to identify every specific source);
‡ *L* = likely, *P*= possible, *U* = unlikely.

Table 4. XRT data analysis results.

Fermi source	XRT source				
	Source	Count rate (10^{-3} cts s^{-1})	$N_{\rm H(Gal)}$ (10^{22} cm^{-2})	Γ	$F(2-10$ keV) (10^{-12} erg cm^{-2} s^{-1})
1FHL J0639.6–1244	single	430.10 ± 24.67	0.299	2.07 ± 0.17	13.1
1FHL J0644.2+6036	single	16.45 ± 0.49	0.065	$2.38^{+0.51}_{-0.56}$	0.26
1FHL J0746.3–0225	#1	28.48 ± 2.63	0.0769	2.64 ± 0.37	0.37
	#2	5.03 ± 1.30	0.0796	–	–
1FHL J1115.0–0701	single	3.08 ± 1.10	0.0348	–	–
1FHL J1129.2-7759	single	331.10 ± 10.05	0.073	1.96 ± 0.08	7.62
1FHL J1223.3+7953	single	5.71 ± 1.40	0.052	–	–
1FHL J1240.4–7150	single	279.70 ± 7.71	0.140	1.96 ± 0.07	7.76
1FHL J1315.7–0730	single	63.56 ± 3.14	0.0308	2.68 ± 0.13	0.56
1FHL J1410.4+7408	#1	1.57 ± 0.57	0.0223	–	–
	#2	2.84 ± 0.79	0.0225	–	–
1FHL J1507.0–6223	single	3.11 ± 1.10	0.419	–	–
1FHL J1856.9+0252[†]	single	2.80 ± 0.38	1.510	[1.8]	0.50
1FHL J2134.6–2130	#1	1.83 ± 0.49	0.0333	–	–
	#2	2.19 ± 0.53	0.0334	–	–
	#3	1.18 ± 0.42	0.0325	–	–
1FHL J2257.9–3644	#1	5.33 ± 1.50	0.0114	–	–
	#2	6.10 ± 1.50	0.0115	–	–

[†] Despite of the poor statistical quality of the XRT data, the X-ray data indicate the presence of an intrinsic absorption $N_{\rm H(intr)} = \left(21.2^{+12.3}_{-8.9}\right)\times10^{22}$ cm^{-2}.